Electronic Supplementary Material (ESI) for Physical Chemistry Chemical Physics.


**Electronic Supplementary Information**

# Achieving High Resolution and Controlling Sensitivity In Spatially Frequency Encoded NMR Spectroscopy: From Theory To Practice

*Bertrand Plainchont, Daisy Pitoux, Ghanem Hamdoun[◊], Jean-Michel Ouvrard, Denis Merlet, Jonathan Farjon and Nicolas Giraud**

# Table of Contents


Table of Contents ..... 2

NMR Experiments ..... 3

Single gradient encoded shaped pulse experiment ..... 3

$\omega_1$-broadband homonuclear decoupled experiments ..... 3

G-SERF experiments ..... 4

NMR Simulations ..... 4

Spatial properties of gradient encoded pulses ..... 6

Resolution and sensitivity in gradient encoded $^1$H spectra ..... 8

Simulated gradient encoded $^1$H spectra ..... 8

Experimental gradient encoded $^1$H spectra ..... 9

Construction of model curves for sensitivity ratios (Fig. 7 in main text) ..... 10

Pure shift NMR implemented with SFE ..... 11

Spatial properties of gradient encoded pure shift evolutions ..... 11

2D $\omega_1$-homonuclear decoupled spectra with a gradient encoded Rsnob refocusing pulse ..... 12

References ..... 13

## NMR Experiments

Experiments were carried out on 10 mg of 3-hydroxy-4,4,4-trichlorobutyric β-lactone **1** dissolved in 700 μL of deuterated chloroform.

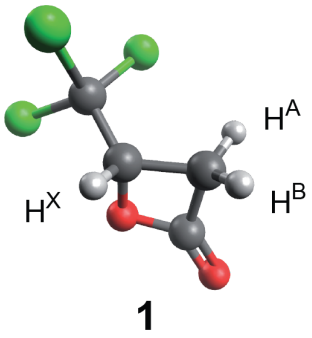


**Fig. S1.** The structure of the model ABX spin system **1.**

NMR spectra were acquired at 300 K on a Bruker AVANCE II NMR spectrometer operating at 14.1 T, equipped with a 5 mm 2H-1H/19F cryoprobe with *z* field gradient coil of maximum gradient strength 53.7 $G.cm^{-1}$.

### Single gradient encoded shaped pulse experiment

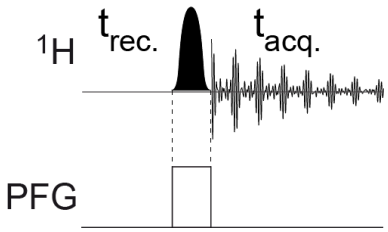


**Fig. S2.** The single gradient encoded pulse sequence. The delays $t_{rec.}$ and $t_{acq.}$ are the recovery and the acquisition times, respectively. The black ellipsoidal shape on the proton channel ($^1$H) corresponds to a shaped excitation pulse. The white rectangular bar on the pulsed-field gradient (PFG) channel refers to the application of a rectangular shaped *z* field gradient.

### $\omega_1$-broadband homonuclear decoupled experiments

The phase cycle is $\phi_1$ = (x, -x), $\phi_2$ = (x, x, -x, -x), $\phi_3$ = (x, x, -x, -x), $\phi_4$ = (x, y, -x, -y), and $\phi_{rec}$ = (-y, -x, -y, -x). An E-BURP-2 shape (resp. RE-BURP/R-SNOB) was used for the excitation (resp. refocusing) pulses of duration 60 ms (resp. 60 ms/20 ms). The gradient amplitude used to generate the spatial frequency encoding was 1% of the maximum gradient strength available. A sine-shaped gradient pulse of duration 1 ms and 10% of the maximum gradient

strength available, followed by a recovery delay of 0.15 ms was used in the *z* filter. For each of the 512 increments in $t_1$, free induction decays of 8192 points were acquired, with 4 scans and recycle delays between scans of 1.5 s. The direct and indirect spectral windows were both set to 2500 Hz. A phasable 2D map was obtained using the Time-Proportional Phase Incrementation Method. Experimental data were processed by using zero-filling up to 1024 points in $t_1$ and 16384 points in $t_2$, apodization with an exponential function using a line broadening of 1.0 and 1.5 Hz, and automatic baseline correction in direct and indirect dimensions, respectively. For simulated data, the natural linewidth of each proton signal was assumed to be the same, and was accounted for by increasing the line broadening by 0.7 Hz, which corresponds to the average observed linewidth on the standard $^1$H spectrum.

### G-SERF experiments

The phase cycle is $\phi_1$ = (x, -x), $\phi_2$ = (x, x, -x, -x), $\phi_3$ = (x, -x, -x, x), $\phi_4$ = (x, y, -x, -y), and $\phi_{rec}$ = (-y, x, -y, x). An E-BURP-2 shape (resp. RE-BURP/R-SNOB and Time reversal E-BURP-2) was used for the excitation (resp. refocusing and flip-back) pulses of duration 60 ms (resp. 60 ms/20 ms and 60 ms). The offset of the non-encoded soft π pulse was set at the desired resonance frequency of the proton spin whose coupling network was probed. The gradient amplitude used to generate the spatial frequency encoding was 1% of the maximum gradient strength available. A sine-shaped gradient pulse of duration 1 ms and 10% of the maximum gradient strength available, followed by a recovery delay of 0.15 ms was used in the *z* filter. For each increment in $t_1$, free induction decays of 4096 points were acquired, with 4 scans and recycle delays between scans of 1.5 s. The spectral windows were set to 2500 Hz in the direct domain and 25 Hz in the indirect domain. A phasable 2D map was obtained using the Quadrature Sequential Mode. Data were processed by using zero-filling up to 128 points in $t_1$ and 8192 points in $t_2$, apodization with an exponential function using a line broadening of 1.0 Hz and 0.3 Hz, and automatic baseline correction in the direct and indirect dimension, respectively.

## NMR Simulations

For the simulation of the spin system **1**, chemical shifts of spins $H^A$, $H^B$ and $H^X$ are 3.6169 ppm, 3.7425 ppm, and 5.0180 ppm respectively. Homonuclear scalar couplings are $J^{A\text{-}B}$ = -17.06 Hz, $J^{A\text{-}X}$ = 3.72 Hz, and $J^{B\text{-}X}$ = 5.75 Hz. These values were adjusted by fitting carefully the simulated $^1$H spectrum to experimental data recorded at 14.1 T. The simulations were

performed using the SpinDynamica program[1] under Mathematica 9.0[2] on a computer equipped with an 8 Intel Xeon processors E5-2609v2 2.5GHz and 32 Go DDR3 memory.

In all simulations, the encoding gradient strength was set so as to encode the entire spectral width. For the simulations allowing for visualizing the magnetization profile, the spatial frequency encoding gradient was modeled by dividing the sample into 401 (Figs. 2, 3, 8 and 9) or 1201 virtual slices (Figs 4, 6, 10 and 13). For 1D spectra, the same parameters as the corresponding experiments were used for simulations and the encoding gradient was modeled by dividing the sample into 201 virtual slices. For 2D spectra, only the virtual slices around positions encoded at $\nu^A$, $\nu^B$ and $\nu^X$ were computed. It was checked that the resulting spectrum is similar to the one obtained by computing the whole virtual sample when a reduced swept width of 450 Hz (resp. 330 Hz) is considered around $\nu^A$ and $\nu^B$ (resp. $\nu^X$). The simulated 1D and 2D data were processed with zero-filling and apodization with an exponential function in the direct and indirect dimensions to adjust the lineshape to corresponding experimental spectra.

For a given pulse sequence, the local density operator $\rho(z,t)$ has been computed for selected virtual slices at positions $z$. The NMR signal issued from the calculations was digitized following the desired quadrature scheme and the resulting real and imaginary parts of the FID were injected into a dataset that is compatible with further processing using the ©Bruker's TopSpin™ software.

## Spatial properties of gradient encoded pulses

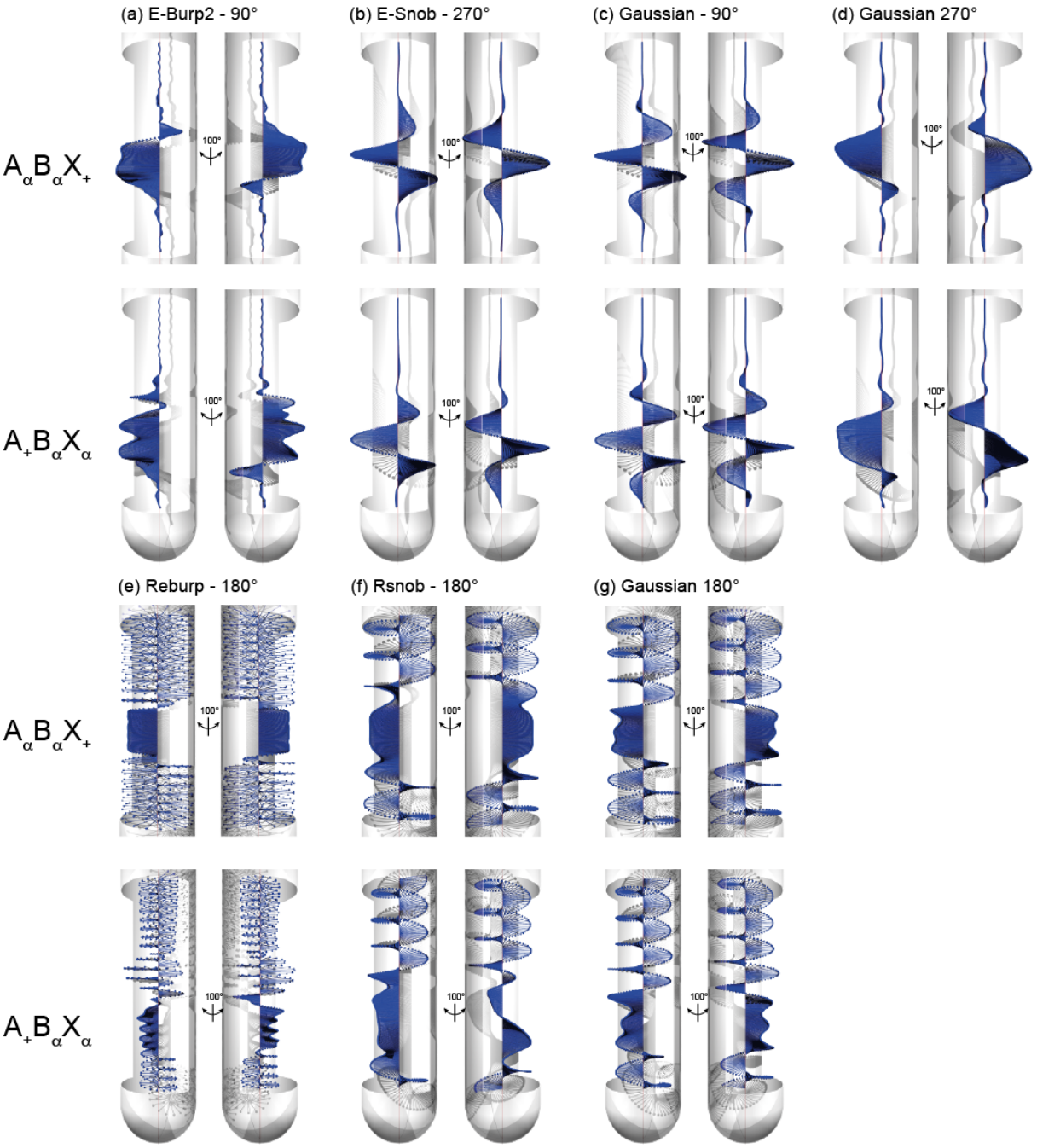


**Fig. S3.** The spatial variation of the magnetization along the *z* axis calculated at the end of a gradient encoded selective excitation (a, b, c, d) and refocusing (e, f, g) pulse, for the $A_+B_\alpha X_\alpha$ and $A_\alpha B_\alpha X_+$ coherences of $H^A$ and $H^X$. E-Burp2 90° (a), E-Snob 270° (b), Gaussian 90° (c), Gaussian 270° (d), Reburp (e), Rsnob (f) and Gaussian 180° (g) shaped pulses of respective duration 60, 20, 20, 20, 60, 20 and 20 ms were used to perform the selective irradiations. For refocusing pulses, the initial state is a transverse magnetization in all slices.

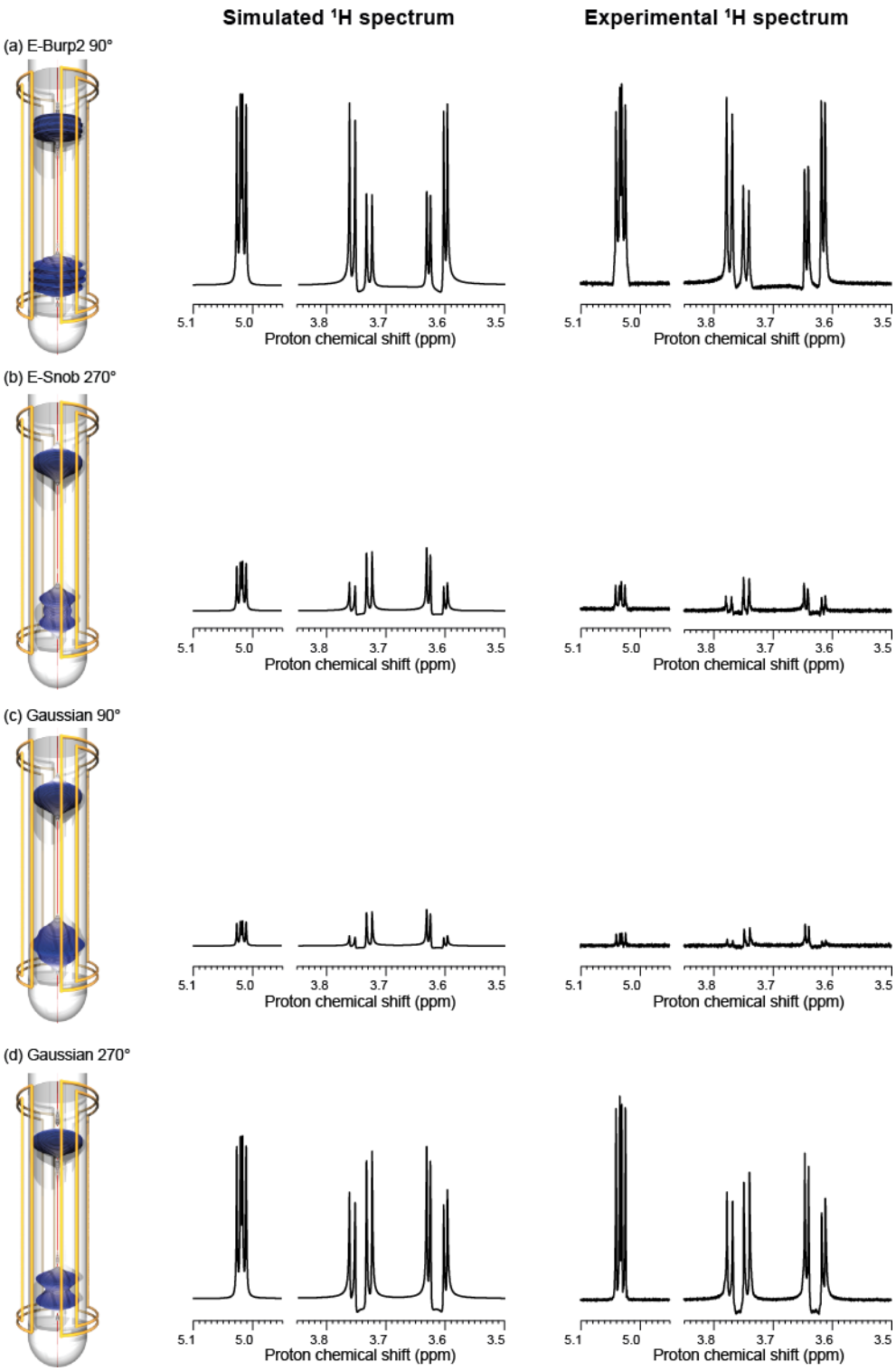


**Fig. S4.** The integration profiles, and the corresponding simulated and experimental gradient encoded $^{1}$H spectra that were generated for a gradient encoded excitation using E-Burp2 90° (a), E-Snob 270° (b), Gaussian 90° (c) and Gaussian 270° (d) of respective duration 60, 20, 20 and 20 ms.

# Resolution and sensitivity in gradient encoded $^{1}$H spectra

## Simulated gradient encoded $^{1}$H spectra

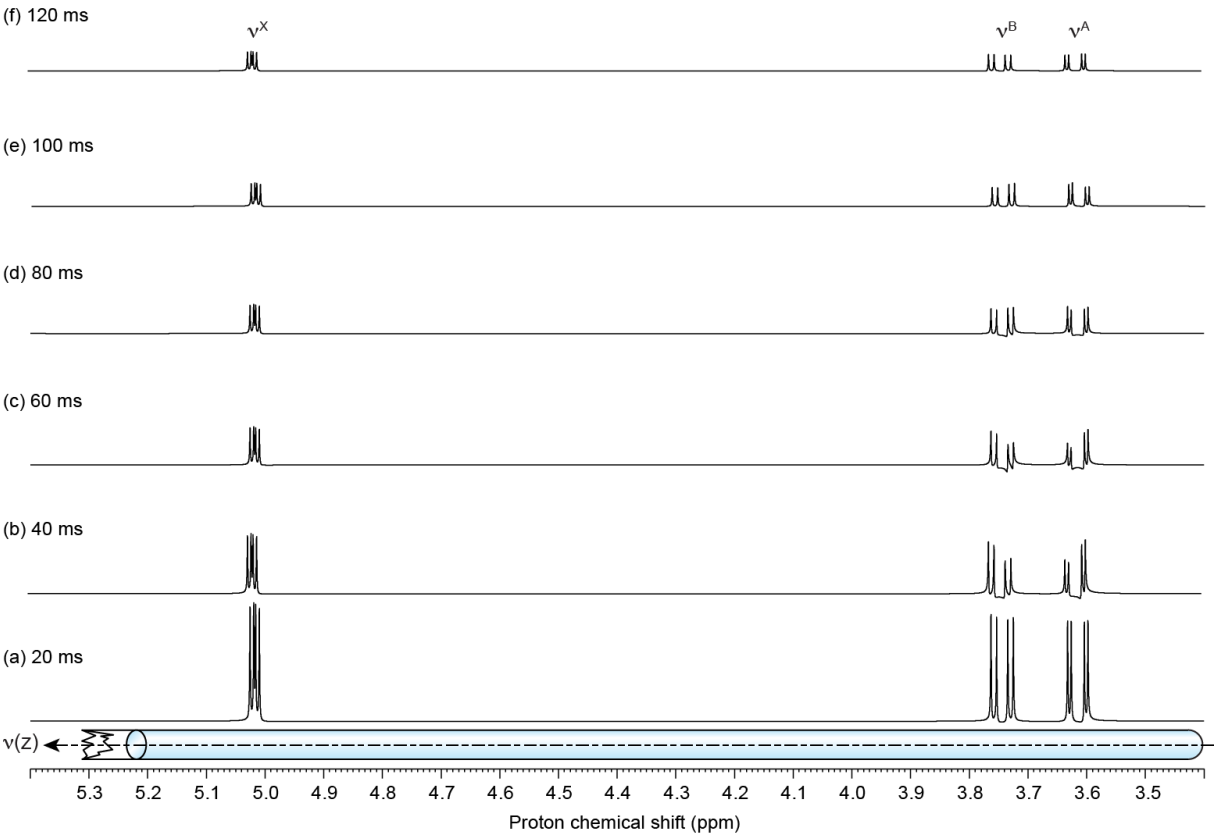


**Fig. S5.** Simulated gradient encoded $^{1}$H spectra of **1** calculated for an E-BURP2 shaped pulse of duration (a) 20 ms, (b) 40 ms, (c) 60 ms, (d) 80 ms (e) 100 ms and (f) 120 ms. The encoded spectral width was set to 3772.6 Hz.

## Experimental gradient encoded $^{1}$H spectra

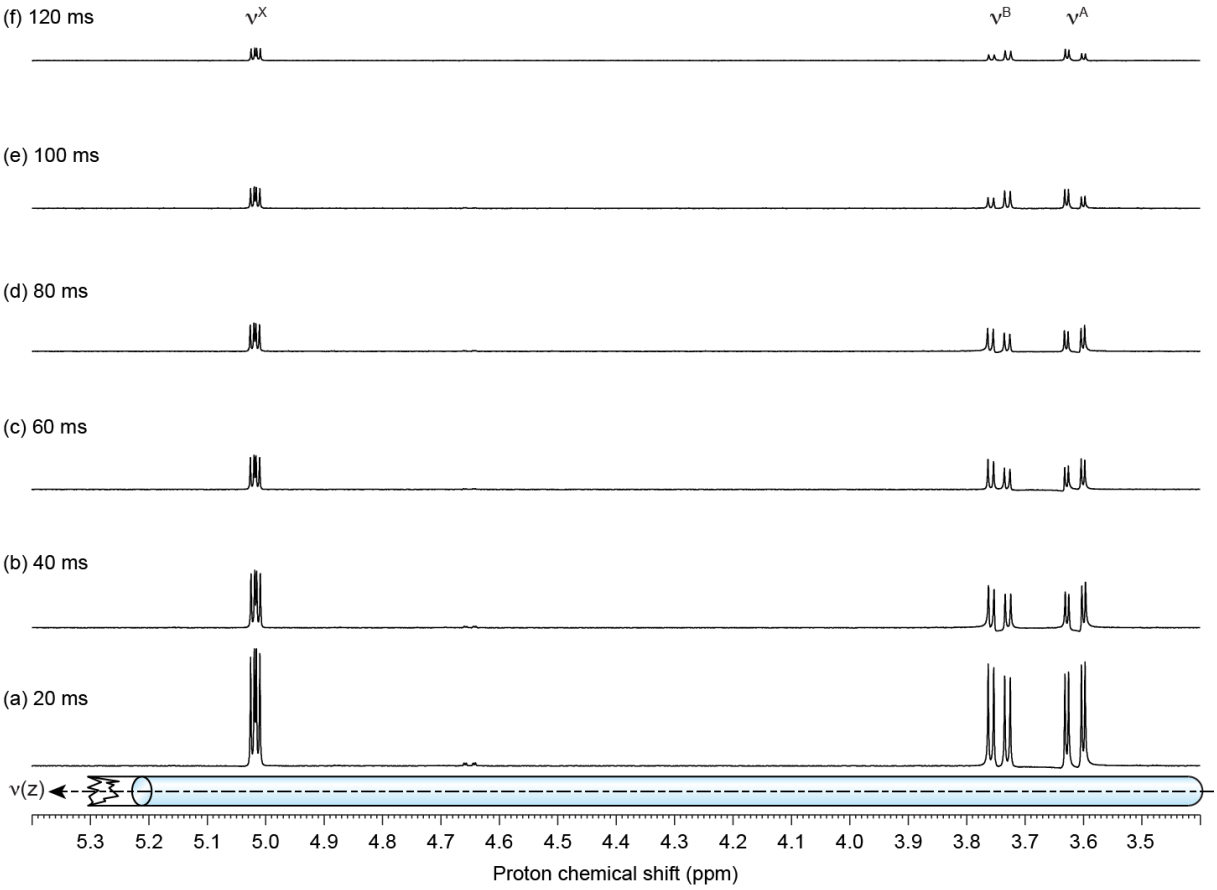


**Fig. S6.** Experimental gradient encoded $^{1}$H spectra of **1** acquired for an E-BURP2 shaped pulse of duration (a) 20 ms, (b) 40 ms, (c) 60 ms, (d) 80 ms (e) 100 ms and (f) 120 ms. The encoded spectral width was set to 3772.6 Hz.

## Construction of model curves for sensitivity ratios (Fig. 7 in main text).

We have used a model initially proposed by Pell and Keeler to describe the evolution of the sensitivity ratio in a gradient encoded experiment.[3] it is assumed that if a spectral width *SW* is encoded by a pulsed field gradient along the whole height of the sample detected by the receiver coil, then the amount of signal generated by an encoded "slice" is proportional to the spectral bandwidth of the selective pulse $\Omega_B$, yielding a sensitivity ratio of the order of:

$$\frac{I^X_{encoded}}{I^X_{ref}} = \frac{\Omega_B}{SW} \tag{1}$$

For the E-Burp2 pulse studied in this work, the resulting model curve was adjusted to the simulated ratios by taking a bandwidth of 87 Hz at 60 ms, and assuming that this bandwidth is proportional to the inverse of the pulse duration $\tau_p$. The encoded spectral width *SW* is identical in the simulation and in the experiment. It was experimentally determined from the relation:

$$SW = \frac{\gamma_H \cdot G_z \cdot h}{2\pi} \tag{2}$$

where $\gamma_H$ is the gyromagnetic ratio of proton, $G_z$ is the strength of the magnetic field gradient, and *h* is the height of the receiver coil. The maximum gradient strength was carefully determined through diffusion measurements performed on a reference sample and is equal to 53.7 G.cm$^{-1}$. The encoding gradient was set to 1 % of its maximum strength. The height of the receiver coil was estimated at 1.65 cm. The encoded spectral width was thus evaluated at 3772.6 Hz. An adapted model accounting for a transverse relaxation process during the selective pulse was used to fit experimental data:[4]

$$\frac{I^X_{encoded}}{I^X_{ref}} = \frac{\Omega_B}{SW} \cdot e^{-\tau_P/T_2} \tag{3}$$

where $\tau_P$ is the pulse duration, and $T_2$ is the transverse relaxation time of the encoded proton nucleus. For $H^X$, $T_2$ was experimentally estimated at 430 ms, whereas a longitudinal relaxation time $T_1$ of 6.62 s was determined by a standard inversion -recovery experiment, which allows for neglecting the contribution of transverse relaxation during the gradient encoded pulse, and accounting only for transverse relaxation.[4, 5] This value was used successfully in the model curve to fit experimental sensitivity ratios shown in Figure 7 in the main text.

## Pure shift NMR implemented with SFE

### Spatial properties of gradient encoded pure shift evolutions

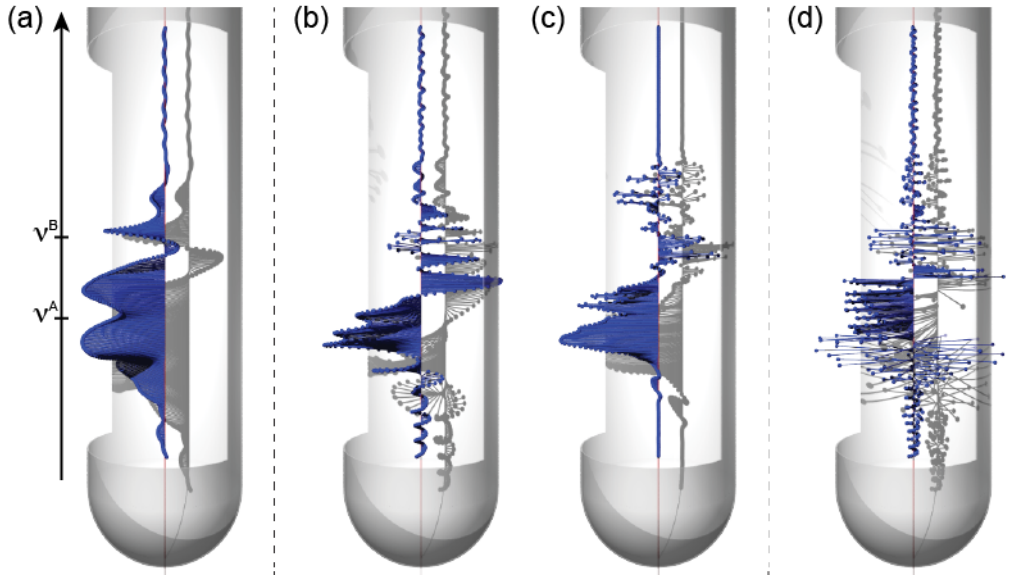


**Fig. S7.** The variation of the magnetization along the *z* axis calculated in each virtual slice for the $A_+B_aX_a$ coherence of $H^A$ at 14.1 T, at the end of the gradient encoded excitation step (a), after the δ-resolved evolution block (b, d) and after the z-filter (c). An E-BURP2 shaped pulse of duration 60 ms was used to perform the selective excitation. A Re-BURP shaped pulse of duration 60 ms (b, c) and 120 ms (d) was used for the selective refocusing.

## 2D $\omega_1$-homonuclear decoupled spectra with a gradient encoded Rsnob refocusing pulse

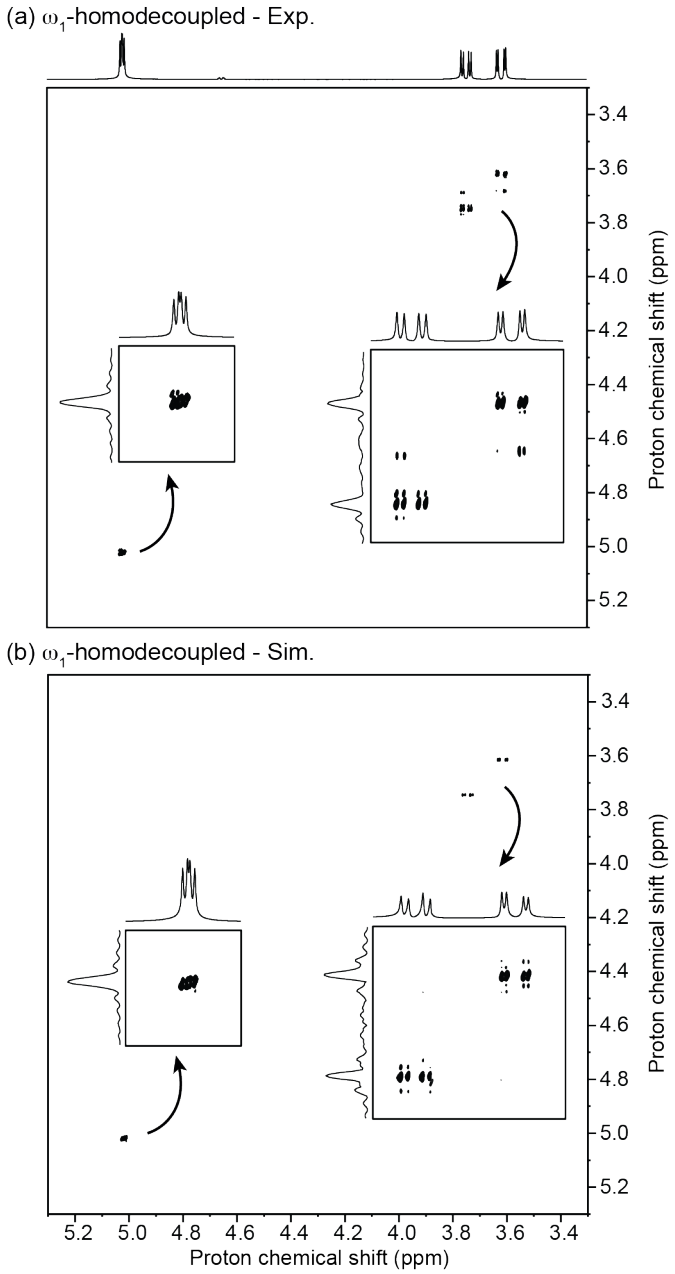


**Fig. S8.** Experimental (a) and calculated (b) 2D $\omega_1$-homodecoupled spectra of **1** recorded with an E-BURP2 pulse of 60 ms during the gradient encoded excitation step, and Rsnob pulses of 20 ms during the *pure shift* block. 512 points were acquired in the indirect domain. The spectral width encoded by the encoding pulsed field gradient was 3773 Hz (6.29 ppm).

## References


1. SpinDynamica code for Mathematica, programmed by Malcolm H. Levitt, with contributions by Jyrki Rantaharju, Andreas Brinkmann, and Soumya Singha Roy, available at http://www.spindynamica.soton.ac.uk.
2. I. Wolfram Research, Wolfram Research, Inc. , Champaign, Illinois, 9.0 edn., 2012.
3. A. J. Pell and J. Keeler, *J. Magn. Reson.*, 2007, **189**, 293-299.
4. P. J. Hajduk, D. A. Horita and L. E. Lerner, *Journal of Magnetic Resonance, Series A*, 1993, **103**, 40-52.
5. K. Zangger, M. Oberer and H. Sterk, *J. Magn. Reson.*, 2001, **152**, 48-56.